DFT STUDY OF NON-IPR TETRAHEDRAL FULLERENES

Katalin NAGY, Levente Csaba NAGY

Babes-Bolyai University, Faculty of Chemistry and Chemical Engineering

Arany János street 11, Cluj-Napoca, email: levente.nagy@ubbcluj.ro

UNIVERSITATEA BABEŞ-BOLYAI
BABEŞ-BOLYAI TUDOMÁNYEGYETEM
BABEŞ-BOLYAI UNIVERSITÄT
BABEŞ-BOLYAI UNIVERSITY
TRADITIO ET EXCELLENTIA

XXX. Nemzetközi Vegyészkonferencia
Kolozsvár, 2024.

INTRODUCTION

Fullerenes that violate the isolated pentagon rule (IPR) are highly reactive and were obtained either as endo- or exohedral derivatives.[1] The strain energy in fullerenes is heightened by the presence of pentagon triple formations. In this work the ten smallest tetrahedral fullerenes (C_n, labeled **1**–**10**) containing fused triples of pentagonal rings are investigated by means of density functional theory (DFT), along with their nitrogen-doped heterofullerene ($C_{n-4}N_4$, labeled **1N**–**10N**) and exohedral fullerene hydride (C_nH_4, labeled **1H**–**10H**) counterparts.[2] The effect of nitrogen doping and exohedral hydrogenation at the four reactive sites on the electronic and structural properties is analyzed.

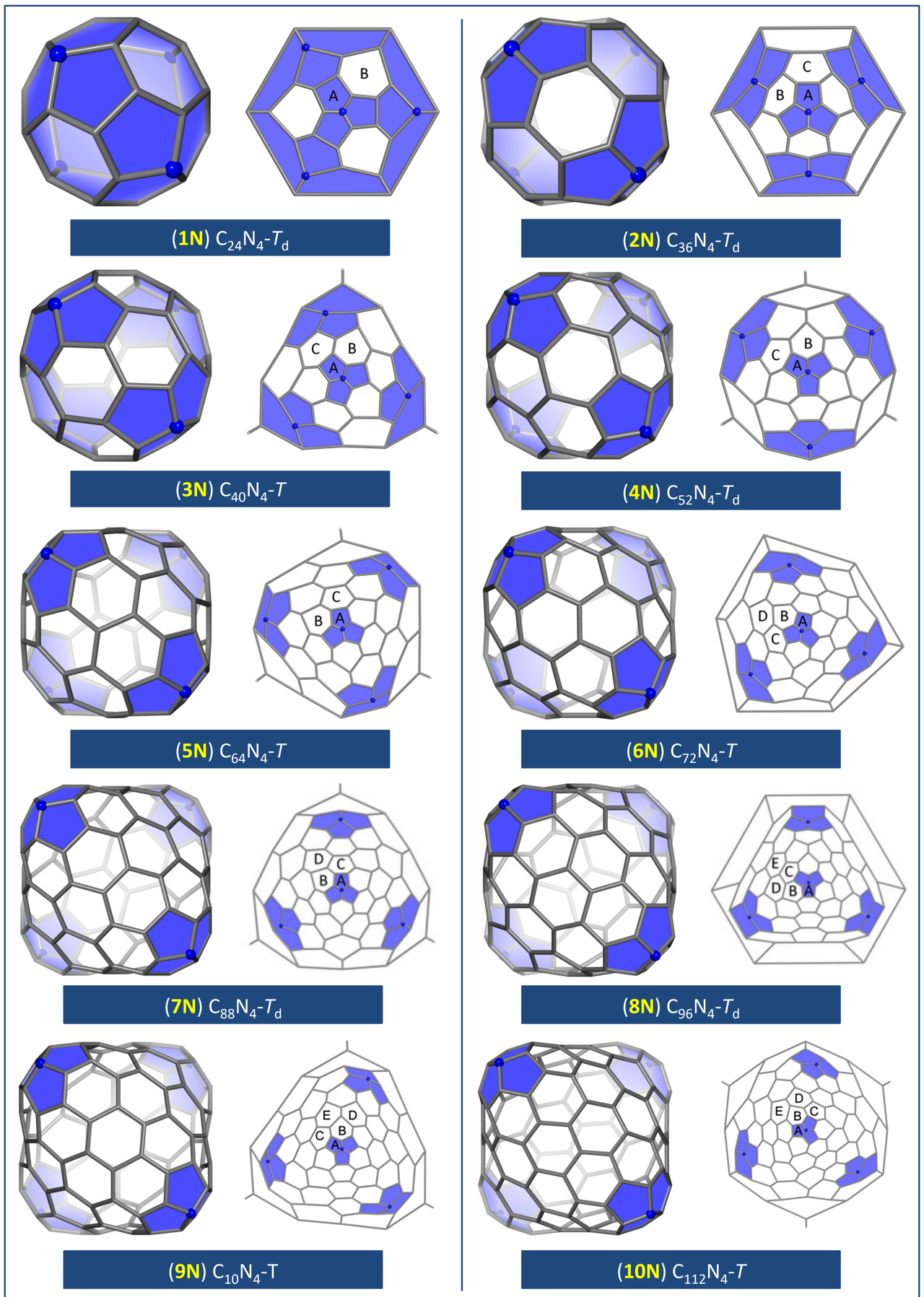

Figure 1. DFT optimized geometries and the corresponding Schlegel projections of the investigated nitrogen-doped tetrahedral heterofullerenes. The positions of the heteroatoms or hydrogen addition sites are indicated with blue spheres. The fused pentagon-triples are highlighted with blue shading. Equivalent rings are labeled accordingly.

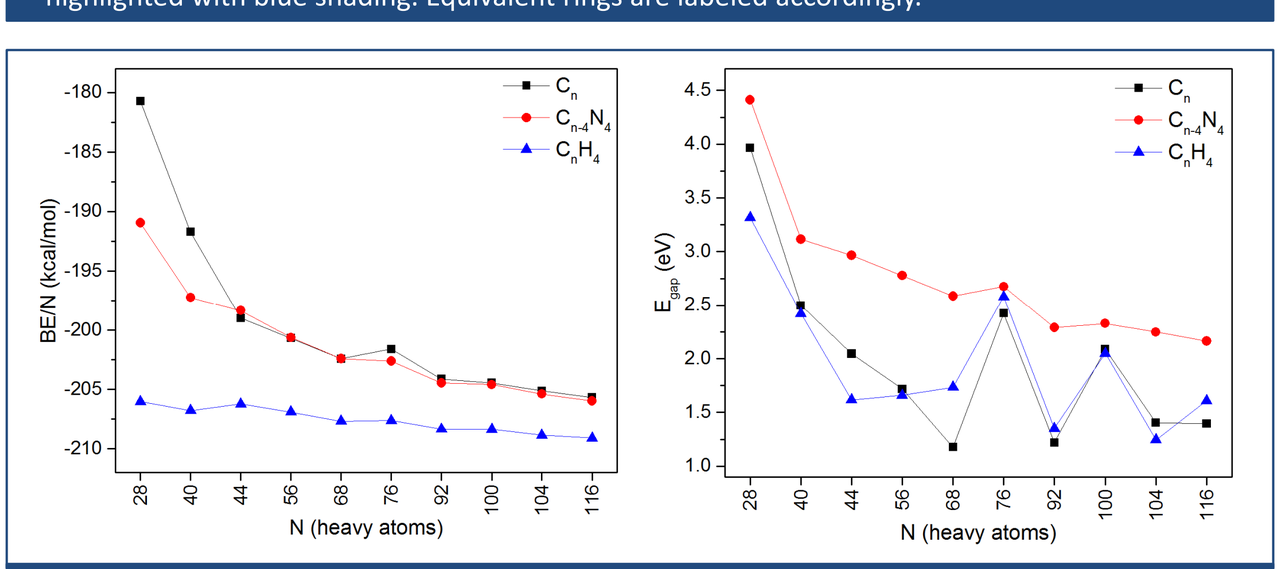

Figure 2. DFT results: binding energies per atom (*BE*/*N*, kcal/mol) and the HOMO–LUMO energy gaps (E_{gap}, eV) as function of the cluster size.

[1] Tan, Y.Z., Xie, S.Y., Huang, R.B. and Zheng, L.S. The stabilization of fused-pentagon fullerene molecules. Nature, **2009**, *1*(6), 450–460.

[2] Nagy, L.C., Nagy, K. Computational Study of Tetrahedral Fullerenes Containing Fused Pentagon-Triples. **2021**, *21*(4), 2419-2426.

COMPUTATIONAL DETAILS

The geometry optimization of each cluster was performed with and without symmetry constraints using B3LYP/6-31G(d). The gauge independent atomic orbital approach was applied to calculate the nucleus-independent chemical shifts (NICS). The global and local aromaticity (**Table 1** and **2**) was assessed by calculating the NICS values at the cage center, at the ring centers (NICS0), as well as 1 Å above and below the rings. The strain energy corresponding to the distortion from planarity of the sp^2 hybridized carbon atoms was also evaluated, according to the π-orbital axis vector (POAV) approach (**Table 4**). All DFT calculations were performed using the Gaussian 09 software package.

According to the Hückel theory, fullerenes C_{28}, C_{40}, C_{76} and C_{100} have an open-shell electronic configuration, where the HOMO orbitals are triply degenerate and are partially filled with two electrons. To preserve their high-symmetry state, the HOMO orbitals of each open-shell fullerene were populated with electrons, and all subsequent computational analyses were conducted on the tetraanionic state.

Table 1. Predicted NICS values (in ppm) of the tetrahedral fullerenes **1**–**10**.

	(1)	(2)	(3)	(4)	(5)	(6)	(7)	(8)	(9)	(10)
O	–34.19	–7.56	–4.68	–28.36	–14.36	–16.50	4.44	–14.95	–11.22	–25.36
A(1)	–3.89	–1.45	1.57	0.39	2.80	0.83	6.33	1.22	4.07	2.30
A0	–12.14	–4.54	0.40	–3.07	6.70	0.37	15.42	–0.12	6.37	1.21
A(–1)	–32.89	–9.64	–7.10	–24.74	–10.84	–14.25	7.29	–14.19	–9.42	–20.55
B(1)	–5.64	–2.29	–0.06	–3.56	–1.66	–0.32	–1.49	–4.21	–2.58	–4.75
B0	–20.92	–9.93	–3.20	–9.50	–4.83	–2.80	–3.54	–11.83	–7.61	–13.40
B(–1)	–35.14	–10.23	–5.03	–26.47	–13.45	–14.47	0.71	–17.91	–12.81	–24.97
C(1)		3.29		–4.74	–1.49	–5.12	1.59	0.52	–0.54	–1.70
C0		3.28		–13.84	–5.47	–13.23	4.40	–1.30	–1.49	–6.13
C(–1)		–5.86		–28.25	–14.08	–20.20	3.98	–12.48	–9.90	–21.41
D(1)						–2.55	2.22	–2.54	–1.34	–4.41
D0						–6.06	5.86	–4.96	–2.21	–9.28
D(–1)						–15.39	3.53	–14.45	–10.92	–23.28
E(1)								–7.65	–3.77	–4.88
E0								–11.41	–5.18	–10.02
E(–1)								–18.76	–11.71	–23.72

Table 2. Predicted NICS values (in ppm) of the tetrahedral azafullerenes **1N**–**10N**.

	(1N)	(2N)	(3N)	(4N)	(5N)	(6N)	(7N)	(8N)	(9N)	(10N)
O	–27.67	–6.98	–21.76	–17.18	–18.61	–18.76	–22.94	–14.75	–23.49	–23.24
A(1)	–3.03	–0.17	–4.63	–4.08	–2.83	0.65	–2.54	1.77	–2.73	–2.17
A0	–9.90	–1.28	–12.23	–10.69	–9.24	0.12	–8.73	2.32	–9.64	–8.35
A(–1)	–26.16	–6.37	–22.27	–19.24	–17.79	–14.57	–21.46	–9.60	–21.58	–21.52
B(1)	–4.99	–3.89	–2.13	–1.67	–2.55	–5.80	–3.44	–4.93	–3.09	–3.51
B0	–19.92	–12.70	–10.37	–7.92	–9.01	–14.92	–11.55	–12.63	–10.93	–12.00
B(–1)	–29.34	–10.75	–21.60	–17.10	–18.77	–22.50	–23.70	–17.71	–23.00	–23.77
C(1)		3.53		–2.28	–2.31	–0.63	–3.37	1.12	–3.11	–2.77
C0		2.91		–8.93	–8.13	–3.90	–9.27	–0.88	–9.08	–8.85
C(–1)		–5.02		–18.03	–18.62	–16.39	–22.69	–11.81	–22.01	–22.08
D(1)						–2.76	–4.83	–1.68	–4.44	–4.83
D0						–6.44	–10.11	–3.15	–9.13	–9.72
D(–1)						–17.15	–21.93	–13.00	–22.29	–22.76
E(1)								–7.86	–4.56	–4.44
E0								–12.84	–9.71	–9.67
E(–1)								–20.15	–22.79	–22.38

Table 3. Topologically equivalent rings in clusters, where the ring labeling corresponds to those used in **Figure 1**.

	C_{28}-T_d	C_{40}-T_d	C_{44}-T	C_{56}-T_d	C_{68}-T	C_{76}-T	C_{92}-T	C_{100}-T_d	C_{104}-T	C_{116}-T
A	12	12	12	12	12	12	12	12	12	12
B	4	6	12	12	12	12	12	12	12	12
C	–	4	–	6	12	12	12	12	12	12
D	–	–	–	–	–	4	12	12	12	12
E	–	–	–	–	–	–	–	4	6	12

Table 4. Global strain energy per carbon atom (kcal/mol) evaluated according to the POAV theory.

	(1)	(2)	(3)	(4)	(5)	(6)	(7)	(8)	(9)	(10)
C_n	16.446	13.993	13.167	11.691	10.823	10.333	9.459	9.183	8.979	8.547
$C_{n-4}N_4$	16.677	13.855	13.413	11.871	10.957	10.347	9.554	9.176	9.051	8.612
C_nH_4	16.012	13.398	13.004	11.566	10.652	10.102	9.349	8.98	8.865	8.448

CONCLUSIONS

The results indicate that the stability increases with the elimination of the energetically unfavorable strain. No correlation was observed between the computed global NICS values and gap energies. With heteroatom substitution the structures maintained or showed a significant increase in the global aromatic character.